Molecular Biology of the Cell
Vol. 20, 4120–4129, September 15, 2009

Phosphorylation of Zona Occludens-2 by Protein Kinase Cε Regulates Its Nuclear Exportation

David Chamorro,* Lourdes Alarcón,* Arturo Ponce,* Rocio Tapia,* Héctor González-Aguilar,† Martha Robles-Flores,† Teresa Mejía-Castillo,* José Segovia,* Yamir Bandala,‡ Eusebio Juaristi,‡ and Lorenza González-Mariscal*

Departments of *Physiology, Biophysics, and Neuroscience and ‡Chemistry, Center for Research and Advanced Studies (CINVESTAV), Mexico, D.F., 07360, Mexico; and †Department of Biochemistry, Faculty of Medicine, Universidad Nacional Autónoma de Mexico, Mexico, D.F. 04510, Mexico

Submitted November 20, 2008; Revised July 6, 2009; Accepted July 9, 2009
Monitoring Editor: Asma Nusrat

Here, we have analyzed the subcellular destiny of newly synthesized tight junction protein zona occludens (ZO)-2. After transfection in sparse cells, 74% of cells exhibit ZO-2 at the nucleus, and after 18 h the value decreases to 17%. The mutation S369A located within the nuclear exportation signal 1 of ZO-2 impairs the nuclear export of the protein. Because Ser369 represents a putative protein kinase C (PKC) phosphorylation site, we tested the effect of PKC inhibition and stimulation on the nuclear export of ZO-2. Our results strongly suggest that the departure of ZO-2 from the nucleus is regulated by phosphorylation at Ser369 by novel PKCε. To test the route taken by ZO-2 from synthesis to the plasma membrane, we devised a novel nuclear microinjection assay in which the nucleus served as a reservoir for anti-ZO-2 antibody. Through this assay, we demonstrate that a significant amount of newly synthesized ZO-2 goes into the nucleus and is later relocated to the plasma membrane. These results constitute novel information for understanding the mechanisms that regulate the intracellular fate of ZO-2.

INTRODUCTION

Zona occludens (ZO)-2 is a 160-kDa protein that localizes at the cytoplasmic plaque of tight junctions (TJs) (Gumbiner *et al*., 1991). ZO-2 belongs to the membrane-associated guanylate kinase protein family whose members are characterized for exhibiting postsynaptic density 95/disc-large/zona occludens (PDZ), Src homology 3, and guanylate kinase (GuK) domains (Gonzalez-Mariscal *et al*., 2000a). ZO-2 also contains an acidic and a proline-rich region that spans from the middle to the carboxy-terminal end. ZO-2 is a scaffold protein that establishes multiple protein–protein interactions (Gumbiner *et al*., 1991; Wittchen *et al*., 1999; Itoh *et al*., 1999a,b; Mattagajasingh *et al*., 2000;Metais *et al*., 2005).

In sparse cultures of epithelial cells, ZO-2 is present at the plasma membrane and at the nucleus (Islas *et al*., 2002). Movement of ZO-2 into the nucleus and out of it depends on nuclear localization signals (NLSs) and nuclear exportation signals (NESs). Canine ZO-2 sequence exhibits two bipartite and three monopartite NLSs whose elimination blocks the nuclear accumulation of this protein in sparse cultures (Jaramillo *et al*., 2004). Four functional NESs are present in canine ZO-2, two localize at PDZ2 and other two at the GuK domain, and the mutation of any of the four NESs is sufficient to induce nuclear accumulation of the protein (Gonzalez-Mariscal *et al*., 2006).

This article was published online ahead of print in *MBC in Press* (http://www.molbiolcell.org/cgi/doi/10.1091/mbc.E08–11–1129) on July 22, 2009.

Address correspondence to: Lorenza González-Mariscal (lorenza@fisio.cinvestav.mx).

Movement to the nucleus can be triggered in confluent monolayers by mechanical injury (Islas *et al*., 2002) or chemical stress induced by treatment with $CdCl_2$ and heat shock (42°C) (Traweger *et al*., 2003). The presence of ZO-2 at the nucleus is regulated by the cell cycle as ZO-2 enters the nucleus at the late G1 phase and leaves the nucleus during mitosis (Tapia *et al*., 2009). This explains why cells found at the G0 phase of the cell cycle, like those in confluent cultures or under serum deprivation, have ZO-2 at the cell borders but not at the nucleus, whereas sparse proliferating cells have ZO-2 at the cell borders as well as in the nucleus. The latter observation has raised the questions of which is the first subcellular destiny of newly synthesized ZO-2 in sparse cultures? And how is the movement of ZO-2 between these locations regulated?

To answer these questions, here we have used diverse strategies including a novel nuclear microinjection assay that allows the analysis of the subcellular fate of newly synthesized ZO-2. We found that a significant amount of ZO-2 goes into the nucleus and that some nuclear ZO-2 is later relocated to the plasma membrane. We also demonstrate that export of ZO-2 from the nucleus is critically regulated by novel (n) PKCε phosphorylation of Ser369 located within the NES-1 of ZO-2.

MATERIALS AND METHODS

Cell Culture

Epithelial Madin-Darby kidney (MDCK) II cells clone A10 between the 60th and 90th passage were grown as described previously (Gonzalez-Mariscal *et al*., 1985). Cells were harvested with trypsin-EDTA and plated at sparse (1×10^5 cells/cm^2) density.

Expression Plasmids and Transfection Assays

Full-length canine ZO-2 introduced into the cytomegalovirus expression plasmid pGW1 (pGW1-HA-ZO-2) was kindly provided by Ronald Javier (Baylor College of Medicine, Houston, TX). Transfections of pGW1-HA-ZO-2 and its derived mutant (Mut.) S369A were done with Lipofectamine 2000 (catalog no 11668-019; Invitrogen, Carlsbad, CA) according to the manufacturer's instructions.

ZO-2 Fusion Proteins

We used a glutathione transferase (GST) fusion protein of the amino-terminal (398–2165 nt) segment of canine ZO-2 (amino-ZO-2-GST) that contains PDZ1, PDZ2, and PDZ3 domains of the molecule. The amino-ZO-2-GST construct described previously by us (Gonzalez-Mariscal *et al*., 2006) as well as its derived mutant S369A were used to transform competent *Escherichia coli* (catalog no. 230196, Artic Express RP competent cells; Stratagene, La Jolla, CA). Protein expression was induced for 24 h at 10°C with 0.5 mM isopropyl β-D-thiogalactoside. Fusion proteins were purified by standard methods.

Generation of ZO-2 Mutant S369A

The QuikChange multisite-directed mutagenesis kit (catalog no 200513; Stratagene) was used according to manufacturer's instructions to produce a serine for alanine mutation at site 369 (S369A) of canine ZO-2. For this purpose, the following primer was used: $_{1486}$TAGTGGTGTTGAGAGAC**GCC**AAG-CAAACGCTCATCAAC$_{1523}$, where the numbers indicate the corresponding nucleotides in ZO-2 canine cDNA, the nucleotide triplet that gives rise to the substitute amino acid is underlined, and nucleotides in bold highlight the nucleotides that differ from the canine ZO-2 sequence. This mutation was done in the expression plasmid pGW1 containing full-length canine ZO-2 (HA-ZO-2 S369A) and in the pGEX-3X plasmid containing the amino-ZO-2-GST construct (amino-ZO-2-GST S369A).

Analysis of the Subcellular Distribution of HA-ZO-2

At different time points taken after transfecting MDCK cells with hemagglutinin (HA)-ZO-2 or HA-ZO-2 Mut. S369A, the cells were fixed and processed for immunofluorescence with a mouse monoclonal immunoglobulin (Ig) G against HA (HA-probe F-7, sc-7392; Santa Cruz Biotechnology, Santa Cruz, CA; dilution 1:50) followed by fluorescein isothiocyanate (FITC)-conjugated goat anti mouse (62-6511; Zymed Laboratories, South San Francisco, CA; dilution 1:100). The observations were initiated at 6 h after transfection (time 0). In all experimental conditions, at each time point the subcellular distribution patterns of HA-ZO-2 were analyzed in 100 transfected cells observed in an Eclipse E600 microscope (Nikon, Tokyo, Japan) by using 60× and 100× objective lenses. The nuclear recruitment index refers to the percentage of transfected cells exhibiting nuclear stain and is integrated by cells displaying nuclear distribution in any of the following patterns: only nuclear (N), membrane and nuclear (M+N), cytoplasm and nuclear (C+N), and cytoplasm, nuclear and membrane (C+N+M) (Figure 1A). The fluorescence images were taken in a confocal microscope (SP2; Leica, Wetzlar, Germany), with argon and helium-neon lasers and using the Leica confocal software.

Nuclear Microinjection Assay

To analyze the departure of ZO-2 from the nucleus, we designed a novel nuclear microinjection assay schematically illustrated in Figures 2A and 3A in which the antibody against ZO-2 is injected into the nucleus of live MDCK cells together with a cDNA HA-ZO-2 construct and rhodaminated albumin. Figure 6A schematically illustrates another microinjection assay done as described previously (Gonzalez-Mariscal *et al*., 2000b) in which the export of ZO-2 GST fusion proteins microinjected into the nucleus is analyzed. In both assays rhodaminated albumin is used as a control to verify that the microinjection was done at the nucleus and that the procedure had not torn the nucleus, allowing the release of its content into the cytoplasm.

The microinjection experiments were done as follows: in the first assay, the nuclei of MDCK cells were microinjected with a solution containing 7 ul of solution A (120 mM KCl, 2.5 mM NaCl, 1 mM $MgCl_2$, and 10 mM HEPES, pH 7.4) containing 1 ul of rhodaminated albumin (catalog no. A23016, Invitrogen; 0.5 mg/ml), 1 ul of a rabbit polyclonal antibody against ZO-2 (catalog no. 71-1400, Zymed Laboratories; 250 μg/ml) or against the K^+ channel Kv3.1b (catalog no. APC-014, Alomone Labs, Jerusalem, Israel; dilution 1 μg/μl), and 1 ul of the cDNA construct of HA-ZO-2 (100 ng/μl) or of the β subunit of the Na^+K^+-ATPase (pCIN4-β1; 1 μg/μl) (Shoshani *et al*., 2005) (generously provided by Dr. Liora Shoshani, Department of Physiology, Biophysics and Neuroscience, CINVESTAV, Mexico City, Mexico). In the second assay, the nuclei of MDCK cells were microinjected with a solution containing 8 ul of solution A containing 1 ul of rhodaminated albumin (0.5 mg/ml) and 1 ul of the GST fusion proteins amino-ZO-2-GST (wild type [WT]) or amino-ZO-2-GST S369A (mutant, S369A) (1 mg/ml of each ZO-2 GST fusion protein). Where indicated the microinjection also included 5 μM PKC inhibitor peptide 19-36 (catalog no. 539560; Calbiochem, Darmstadt, Germany) or 2 μM of the nPKCε translocation inhibitor peptide EAVSLKPT (catalog no. 539522; Calbiochem). Where indicated in both assays, cells were incubated 1 h before microinjection, in media containing 50 nM leptomycin B (LMB) (catalog no. L 2913; Sigma-Aldrich, St. Louis, MO), an antifungal compound that inhibits the nuclear export of proteins by blocking association of NESs with the export receptor CRM1/exportin (Kudo *et al*., 1998).

Microinjection was performed using an IM 300 apparatus (Narishige, Tokyo, Japan) with borosilicate pipettes (Kimax 34500, Kimble Chase, Vineland, NJ) that have a tip diameter 0.2–0.5 μm and a resistance of 3–6 MΩ made with a horizontal Brown/Flaming puller (Sutter p87; Sutter Instrument, Novato, CA). The pipettes were backfilled with 1 μl of a solution containing the samples (group 1: rhodaminated albumin, rabbit polyclonal against ZO-2 or a negative control against channel Kv3.1b and a cDNA construct of full-length HA-ZO-2 or of the negative control β subunit of the Na^+K^+-ATPase; group 2: rhodaminated albumin plus amino-ZO-2 GST fusion proteins [WT or S369A]). After filling, the pipettes were attached to a holder connected to a piezoelectric micromanipulator (PCS500; Burleigh, New York, NY). The microinjection was performed on the nuclei of sparse cells plated 8–12 h before on glass coverslips and was verified by the epifluorescence observation of the injected rhodaminated albumin in an inverted microscope (Diaphot 200; Nikon).

In the first assay, after 3 or 6 h of incubation at 37°C the cells were fixed with 4% paraformaldehyde (PFA) and permeabilized with 0.05% Triton X-100 in phosphate-buffered saline (PBS) and processed for immunofluorescence by using a FITC-labeled polyclonal antibody against rabbit IgG (catalog no. 62-6111, Zymed Laboratories; dilution 1:100), a mouse monoclonal against HA, a polyclonal against mouse coupled to biotin (catalog. no. 62-6540, Zymed Laboratories; dilution 1:200), and streptavidin coupled to cyanine 5 (Cy5) (catalog no. 43-8316, Zymed Laboratories; dilution 1:200) or to FITC (catalog no. 43-4311, Zymed Laboratories; dilution 1:200).

In the second assay, after 6 h of incubation at 37°C the cells were fixed with 4% PFA and permeabilized with 0.05% Triton X-100 in PBS and processed for immunofluorescence by using a mouse monoclonal antibody (mAb) against GST (catalog no. 13-6700, Zymed Laboratories; dilution 1:500) and an FITC-labeled polyclonal antibody against mouse IgG.

Biosynthetic Labeling

Subconfluent MDCK cells were incubated for 3 h with 50 μg/ml cycloheximide (CHX), an inhibitor of protein synthesis. After being washed twice with PBS the monolayers were incubated in methionine- and cysteine-free DMEM (catalog no. 010909, In Vitro, Mexico D.F.) containing 4 mM glutamine, 5 μg/ml insulin, and 5% (vol/vol) dialyzed fetal bovine serum and labeled with 200 μCi of Easy Tag Express protein labeling mix [^{35}S]Met/Cys (PerkinElmer Life and Analytical Sciences, Boston, MA) for different times (3, 6, and 9 h). The radioactive medium was removed, and the cells were washed three times with ice-cold PBS and treated with a lysis buffer (10 mM Tris-HCl, pH 7.6, 150 mM NaCl, 1% [wt/vol] sodium deoxycholate, 0.1% [wt/vol] SDS, 1% [vol/vol] NP40, and 1 mM phenylmethylsulfonyl fluoride [PMSF]) containing the protease inhibitor cocktail Complete (Roche Diagnostics, Mannheim, Germany). From these cell lysate, nuclear and membrane fractions were isolated using the Compartmental protein extraction kit (catalog no. 2145; Millipore Bioscience Research, Temecula, CA). The amount of protein in each fraction was quantified, and 250 μg of each cell fraction was used for ZO-2 immunoprecipitation. We then measured, in an LS 6500 multipurpose scintillation counter (Beckman Coulter, Fullerton, CA), the radioactive counts present in 250 μg of nuclear and membrane fractions and in the ZO-2 IP derived from them.

Immunoprecipitation of ZO-2 from the Nuclear and Membrane Fractions of Epithelial Cells

We transferred 250 μg of nuclear and membrane fractions derived from sparse MDCK cells to Eppendorf tubes and vortexed for 40 s. After being gently agitated for 1 h at 4°C, the solution was passed 20 times through a 1-ml syringe. Next, the extracts were clarified with 100 μl of protein A-Agarose pearls (catalog no. 11 134 515 001; Roche Diagnostics) for 1 h at 4°C. After 10 min of centrifugation at 4°C at 1300 × *g*, supernatants were recovered and incubated overnight at 4°C with 2.5 μg of polyclonal antibody against ZO-2 under continuous rotation. Next, we added 100 μl of protein A-Agarose pearls and incubated for 1–3 h at 4°C at constant agitation. After centrifugation at 1300 × *g* for 10 min, the immunoprecipitates were processed according to the protein A-Agarose pearls manufacturer's instructions. The pellets were then solubilized in 100 μl of radioimmunoprecipitation assay (RIPA) buffer (10 mM Tris-HCl, pH 7.6, 150 mM NaCl, 1% NP40, 1.0% sodium deoxycholate, 0.1% SDS, 0.4 mg/ml PMSF, and the protease inhibitor cocktail Complete) and 1× electrophoresis sample buffer and boiled for 10 min. Samples were then centrifuged for 15 min at 4°C and 9000 × *g* to eliminate the protein A-Agarose pearls. The supernatants were then placed in glass vials containing scintillation liquid and measured in an LS 6500 multipurpose scintillation counter (Beckman Coulter).

Coimmunoprecipitation of Protein Kinase Cε with ZO-2

ZO-2 was immunoprecipitated from sparse monolayers of MDCK cells transfected previously with HA-ZO-2 or mutated HA-ZO-2 (S369A). In brief, two 60-cm^2 culture plates containing 1 × 10^5 cells/cm^2 were washed three times

with PBS containing 0.5 mg/ml PMSF and the protease inhibitor cocktail Complete. The monolayers were then bathed with 500 μl of RIPA buffer and scrapped with a rubber policeman. The solution obtained was then transferred to an Eppendorf tube and vortexed for 40 s. After being gently agitated for 1 h at 4°C the solution was passed 10 times through a 1-ml syringe. Next, the cellular extract was treated as above described, for the immunoprecipitation of transfected ZO-2 with a specific mAb against HA and protein A-Agarose pearls. Finally, the ZO-2 inmunoprecipitates were electrophoresed onto 12% polyacrylamide-SDS gels.

Protein Blotting

Proteins were quantified and the samples were diluted (1:1) in treatment buffer (125 mM Tris-Cl, 4% SDS, 20% glycerol, and 10% 2-mercaptoethanol, pH 6.8), run in 8% polyacrylamide gels, and transferred to polyvinylidene difluoride membranes (Hybond RPN303F; GE Healthcare, Little Chalfont, Buckinghamshire, United Kingdom).

Blotting was performed with mouse monoclonal antibodies against HA (HA-probe F-7, sc-7392, Santa Cruz Biotechnology; dilution 1:1000) or anti-conventional (c)PKCβ2 (sc-13149, Santa Cruz Biotechnology; dilution 1:1000) or with a rabbit polyclonal anti-nPKCε (sc-214, Santa Cruz Biotechnology; dilution 1:1000). Peroxidase-conjugated goat IgG anti-mouse IgG (62-6420, Zymed Laboratories; dilution 1:3000) and goat anti-rabbit IgG (A9169, Zymed Laboratories; dilution 1:3000) were used as secondary antibodies, followed by a chemiluminescence detection system (ECL+PLUS, RPN 2132; GE Healthcare).

Treatment with Drugs

All the drugs were added to the cells during the last 2 h of each experimental time point. Bryostatin 1 (catalog no. ST-103; BIOMOL Research Laboratories, Plymouth Meeting, PA) was dissolved and kept at −20°C as a 100 μM stock prepared in dimethyl sulfoxide (DMSO). The stocks of other drugs dissolved in DMSO were kept at 4°C: 1 mM Gö 6976 (catalog no. 365250; Calbiochem), 40 μM Ro-31-8220 (catalog no. 557520; Calbiochem), and 10 mM rottlerin (catalog no. 557370; Calbiochem). In all cases, the final concentration of DMSO was 0.1%, a nonharmful concentration for these monolayers.

Leptomycin B (catalog no. L 2913; Sigma-Aldrich) was dissolved in ethanol and maintained as a 100 μM stock at −20°C. In all cases, the final concentration of ethanol was 0.01%, a nondamaging concentration for MDCK cells.

Protein Kinase C Immune Complex Kinase Assay

This assay was performed as described previously (Robles-Flores *et al*., 2002). In brief, aliquots of 1 ml of partially purified (mixture of α, β, δ, ε, θ, ζ, and μ isoforms obtained from rat hepatocytes) and concentrated PKC (1 mg/ml) were incubated in the presence of phosphatase inhibitors (10 mM β-glycerophosphate, 1 mM Na_2VO_4, 11 mM NaF, 10 mM sodium pyrophosphate, and 0.2 mg/ml phosphoserine) and in the absence of 2-mercaptoethanol, with 1 μg/ml isozyme-specific nPKCε antibody for 1 h at 4°C with gentle shaking. Then, 20 μl of protein A-Sepharose (30%; Calbiochem) was added, and incubation was continued for 1 h. Immune complexes were then washed three times with buffer A (50 mM Tris-HCl, 0.6 M NaCl, 1% Triton X-100, and 0.5% NP40, pH 8.3) supplemented with 0.1 mg/ml trypsin inhibitor and 1 mM PMSF and one time with kinase buffer (20 mM Tris-HCl, pH 7.5, 10 mM $MgCl_2$, 0.5 mM $CaCl_2$, and 50 mM 2-mercaptoethanol). Kinase activity was initiated by resuspending the immunoprecipitates in 50 μl of assay mixture (kinase buffer plus 20 μg/ml phosphatidylserine, 0.8 μg/ml 1,2-diolein, 10 μM [γ^{32}P]ATP [6000 Ci/mmol], and 200 μg/ml protein substrate [histone H1-IIIS; catalog no. H-4524, Sigma-Aldrich or ZO-2 peptides]). Reactions were allowed to proceed for 20 min at 30°C and were terminated by the addition of 50 μl of SDS-polyacrylamide gel electrophoresis (PAGE) sample buffer. The samples were boiled for 5 min and analyzed by 10% SDS-PAGE and autoradiography. Data were quantified by densitometric analysis performed both in Coomassie-stained gels and the corresponding autoradiographies. The ratio of ^{32}P-labeled protein/dyed protein represents the total specific phosphorylation.

Statistical Analysis

Significance test for difference between proportions was analyzed with the two proportions procedure of the statistical package MINITAB (release 14; Minitab, State College, PA). A minimal level of significance ($p < 0.05$) for Fisher's exact test value was considered significant to reject null hypothesis.

RESULTS

Newly Synthesized ZO-2 Concentrates at the Nuclei of Epithelial Cells

We analyzed by immunofluorescence the fate of newly synthesized ZO-2 in MDCK cells transfected with HA-tagged full-length ZO-2 (HA-ZO-2). The cells displayed several patterns of distribution of HA-ZO-2 that can be classified as follows (Figure 1A): nuclear (N); membrane (M); cytoplasm (C); membrane and cytoplasm (M+C); membrane and nucleus (M+N); cytoplasm and nucleus (C+N); and cytoplasm, nucleus, and membrane (C+N+M).

Figure 1B (filled squares) illustrates how nuclear recruitment of HA-ZO-2 is high (74%) at time 0 (6th h after transfection) and diminishes to 17% by the 18th h. Membrane recruitment of HA-ZO-2 could not be evaluated in the same manner because the strong cytoplasmic staining of ZO-2 present in the C and C+N patterns conceals ZO-2 staining at the cell borders.

Newly Synthesized ZO-2 Relocates from the Nucleus to the Plasma Membrane

To evaluate whether nuclear ZO-2 is later displaced to the plasma membrane, we designed a novel nuclear microinjection assay (Figure 2A), whose results reveal in Figure 2B the presence of ZO-2 at the cell borders (empty arrow), thus indicating that ZO-2 had passed through the nucleus before reaching the plasma membrane. The strong green nuclear stain shown in Figure 2Ba corresponds to the ZO-2 antibody that had been microinjected into the nucleus and not necessarily to the ZO-2 protein present at the nucleus. Therefore, to observe all newly synthesized HA-ZO-2, regardless of its passage through the nucleus, we performed another experiment described in Figure 2Ab. Figure 2Bb shows HA-ZO-2 concentrated at the nucleus in a speckled pattern (full arrow); the perinuclear region (arrowhead), where it is probably being synthesized; and the plasma membrane (empty arrow). The blue stain of HA-ZO-2 present at the plasma membrane colocalizes with the FITC stain that detects native and transfected ZO-2 that passed through the nucleus before reaching the plasma membrane.

To further test whether HA-ZO-2 present at the membrane previously passed through the nucleus, in the next experiment we incubated the cells with LMB (Figure 2Ac). Figure 2Bc shows in blue how HA-ZO-2 concentrates at the nucleus, displays a strong diffuse staining at the cytoplasm and is no longer detectable at the plasma membrane. Therefore, we conclude that most of the newly synthesized ZO-2 travels first to the nucleus and then to the plasma membrane, although we cannot rule out the possibility that a small amount of ZO-2 can reach the plasma membrane directly from the cytoplasm.

Next, we analyzed whether native ZO-2 could be shuttling from the plasma membrane to the nucleus and back to the cell borders by using the protocol described in Figure 2Ad. The images in Figure 2Bd show no green staining at the plasma membrane, indicating that ZO-2 present at the cell borders has not been in contact with the nuclear pool of antibody against ZO-2 and that the amount of newly synthesized native ZO-2 that went from the nucleus to the plasma membrane in the 6-h period studied was so low that remained nondetectable. Together, these microinjection assays indicate that newly synthesized ZO-2 that travels to the nucleus can later be relocated to the plasma membrane.

Next, we performed a set of nuclear microinjection control experiments in which the rabbit antibody against ZO-2 was substituted for an unrelated rabbit IgG corresponding to a rabbit polyclonal against the Kv3.1b channel (Figure 3Aa) or the microinjected cDNA for HA-ZO-2 was replaced for a non–ZO-2 cDNA, corresponding to the cDNA for the β subunit of the Na^+K^+-ATPase (Figure 3Ab). Figure 3Ba illustrates that no ZO-2 stain is present at the cell borders when the antibody against ZO-2 is substituted for an unrelated antibody, and Figure 3Bb shows that the green stain that corresponds to the antibody against ZO-2 remains at the

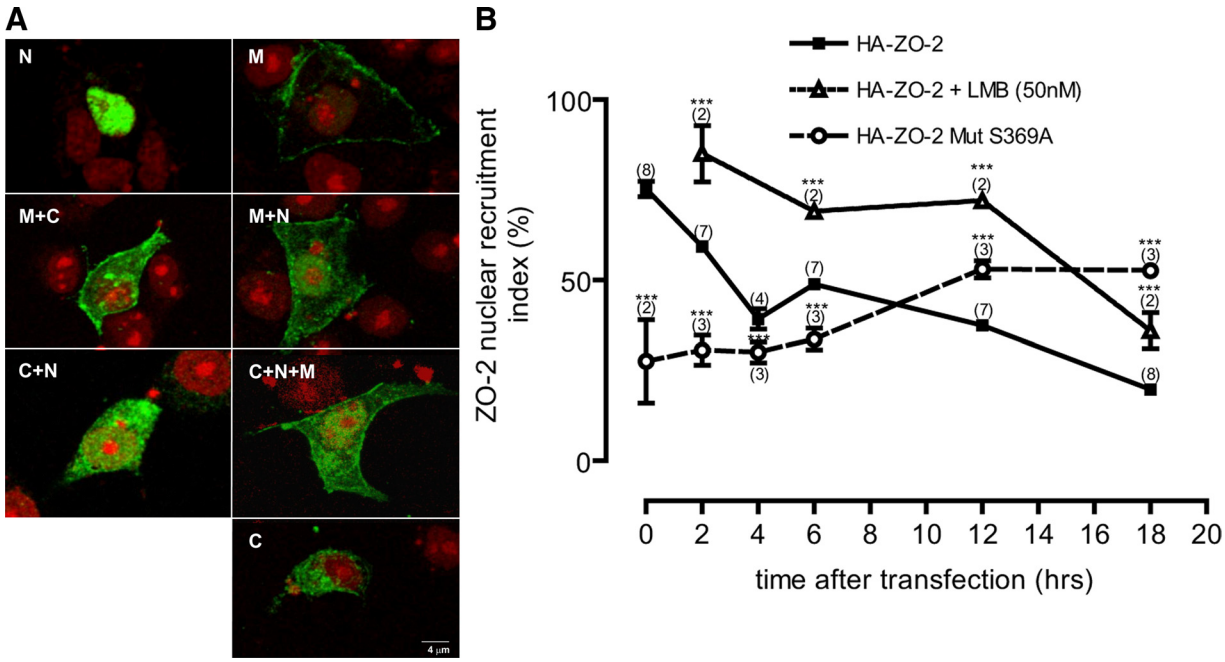

Figure 1. The presence of ZO-2 at the nucleus diminishes with time in a process sensitive to LMB and dependent on ZO-2 Ser369 phosphorylation. (A) Newly synthesized HA-ZO-2 displays several subcellular patterns of distribution in MDCK cells. Nuclei were stained with ethidium bromide (red), and HA-ZO-2 was detected with a specific antibody against HA (green). N, nuclear; M, membrane; C, cytoplasm; M+C membrane and cytoplasm; M+N membrane and nucleus; C+N, cytoplasm and nucleus; and C+N+M cytoplasm, nucleus and membrane. (B) Percentage of cells with nuclear ZO-2 as a function of time. The percentage of cells with nuclear ZO-2 was determined by immunofluorescence using an anti-HA antibody. Monolayers were fixed at the indicated times. Time 0 corresponds to the 6th h after transfection. Experiments were done with cells transfected with full-length HA-ZO-2 without (full squares) or with 50 nM LMB added for the last 2 h (triangles), and with full-length HA-ZO-2 containing a point mutation at Ser369 (HA-ZO-2 Mut. S369A, circles). In parentheses, we indicate the number of independent experiments performed. In each experiment, the distribution pattern of transfected ZO-2 was analyzed in 100 cells for each time point. *$p < 0.05$; **$p < 0.005$; and ***$p < 0.0005$, using a Fisher exact test comparing experimental to control values.

nucleus when no ZO-2 is transfected, confirming the results of Figure 2Bd that indicate that in the time period studied no endogenous ZO-2 is leaving from the nucleus to the plasma membrane or that the amount departing is too low for immunofluorescence detection.

Endogenous ZO-2 Travels to the Nucleus before Reaching the Plasma Membrane

It can be argued that the amount of newly synthesized overexpressed ZO-2 delivered directly to the borders would depend on the number of available binding sites at the borders, which may already be occupied by endogenous ZO-2. Under such condition, overexpressed ZO-2 would accumulate in the nucleus. Therefore, we devised another experiment in which we analyzed the movement of newly synthesized endogenous ZO-2 in cells that had been previously subjected to a 3-h protein synthesis blockade by treatment with 50 μg/ml cycloheximide (Figure 3Ac). In this case, a faint yet detectable signal of ZO-2 is present at the cell borders (Figure 3Bc, arrow). This plasma membrane stain is abolished if the cells are treated with LMB (Figure 3Ad and 3Bd). These results indicate that even when the amount of endogenous ZO-2 is diminished due to a previous protein synthesis blockade, newly synthesized endogenous ZO-2 can travel to the nucleus before reaching the plasma membrane.

A Higher Amount of Newly Synthesized Endogenous ZO-2 Reaches the Nucleus than the Plasma Membrane

We next determined the amount of newly synthesized endogenous ZO-2 that is incorporated to membrane and nuclear fractions in monolayers subjected to 3-, 6-, and 9-h pulses of [^{35}S]Met/Cys. These cultures had been incubated previously for 3 h with cycloheximide. Figure 4A shows that the amount of newly synthesized ZO-2 that incorporates to the plasma membrane is the same with 3-, 6-, and 9-h [^{35}S]Met/Cys pulses. As expected, the amount of [^{35}S]Met/Cys that incorporates to the membrane fraction is two orders of magnitude higher than that present in the ZO-2 IP derived from the membrane fraction. In the nuclear fraction instead, a sharp increase in the amount of [^{35}S]Met/Cys present in the ZO-2 immunoprecipitate (IP) is detected with the 6-h pulse, whereas by the 9th h, the amount has decreased to values similar to those found with the 3-h pulse. The amount of [^{35}S]Met/Cys present in the nuclear fraction is one order of magnitude higher than that found in the ZO-2 IP derived from the nuclear fraction (Figure 4B). More importantly, the amount of counts in the ZO-2 IP derived from the nuclear fraction is significantly higher than that present in the ZO-2 IP derived from the membrane fraction (3 h: 1051 ± 94 vs. 302 ± 139; 6 h: 4871 ± 1548 vs. 234 ± 89; and 9 h: 2306 ± 1628 vs. 281 ± 18). These values are 3.4-, 20.8-, and 8.2-fold higher at 3, 6, and 9 h, respectively. Figure 4C reveals that the ratio of counts from the nuclear ZO-2 IP/nuclear fraction is significantly higher than the ratio of counts from the membrane ZO-2 IP/membrane fraction with 3-, 6-, and 9-h pulses. Together, these results indicate that once protein synthesis is triggered, a significantly higher amount of newly synthesized ZO-2 reaches the nucleus than the plasma membrane. Although the amount of ZO-2 at the membrane is maintained relatively constant, the

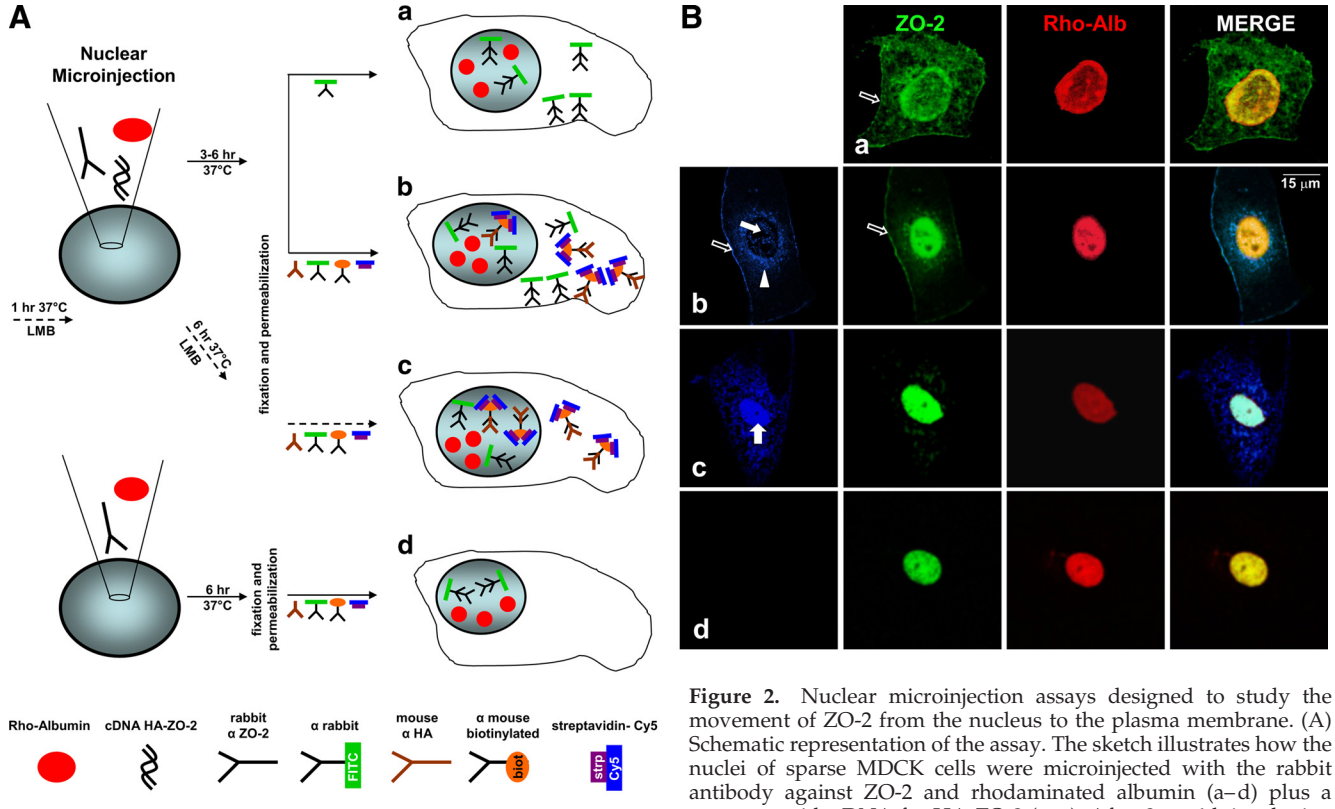

Figure 2. Nuclear microinjection assays designed to study the movement of ZO-2 from the nucleus to the plasma membrane. (A) Schematic representation of the assay. The sketch illustrates how the nuclei of sparse MDCK cells were microinjected with the rabbit antibody against ZO-2 and rhodaminated albumin (a–d) plus a construct with cDNA for HA-ZO-2 (a–c). After 3- to 6-h incubation at 37°C, the cells were fixed and processed for immunofluorescence with an FITC-coupled antibody against rabbit IgG (a–d) plus a mouse antibody against HA, a biotinylated antibody against mouse IgG, and Cy5 coupled streptavidin (b–d). In c, the culture was treated with 50 nM LMB 1 h before the microinjection and kept with LMB until the cells were fixed. (B) Immunofluorescence obtained from the nuclear microinjection assays. From a–d, it can be observed that rhodaminated albumin remains confined to the nucleus, indicating that the microinjection had not ragged the nucleus, allowing leakage of the injected compounds. a, ZO-2 can travel from the nucleus to the plasma membrane. Green staining at the cell borders indicates that ZO-2 previously passed through the nucleus where it was labeled with the anti ZO-2 antibody. b, newly synthesized HA-ZO-2 (blue) is present at the nucleus in a speckled pattern (full arrow), at the perinuclear region (arrowhead) and the plasma membrane (empty arrow). At the cell borders HA-ZO-2 stain (blue) colocalizes (see merge) with the FITC stain (green) that detects native and transfected ZO-2 that has passed through the nucleus. c, when the nuclear export of ZO-2 is blocked with LMB, no green staining is detected at the plasma membrane. Newly synthesized HA-ZO-2 concentrates at the nucleus (arrow) and exhibits a strong and diffuse cytoplasmic staining (blue). In d, no green staining is detected at the cell borders, indicating that native ZO-2 is not shuttling from the membrane to the nucleus and vice versa. Rho, rhodamine; Alb, albumin.

nucleus seems to serve as a cellular ZO-2 reservoir, whose ZO-2 content is subject to drastic variations with time.

Recruitment of ZO-2 to The Nucleus Is High after Transfection but Diminishes with Time in a Process Sensitive to Leptomycin B and Dependent of ZO-2 Ser369 Phosphorylation

Next, we studied how the nuclear exportation of ZO-2 is regulated. Figure 1B illustrates how in cultures where LMB was added, the percentage of cells displaying HA-ZO-2 at the nucleus is significantly higher than in control monolayers at each time point, indicating that the exportation of HA-ZO-2 from the nucleus is a continuous process regulated by CRM1/exportin.

Previously, through a nuclear microinjection assay, we had shown that ZO-2 NES-1 could not export the reporter protein ovalbumin (Jaramillo *et al.*, 2004), unless a phosphomimetic mutation was performed on the putative PKC phosphorylation site, located at Ser369 (Gonzalez-Mariscal *et al.*, 2006). This observation prompted us to analyze the impact of Ser369 phosphorylation on the nuclear export of full-length ZO-2. Figure 1B (circles) shows how when Ser369 is replaced by Ala (S369A HA-ZO-2), the percentage of cells exhibiting ZO-2 at the nucleus 6 h after transfection (time 0), is significantly lower than in control monolayers (control 74% vs. S369A 27%); yet, this initial percentage instead of diminishing with time as happens with control monolayers, experiences an increase to 53% by the 12th h and remains stable for at least 12 more hours. This result strongly suggests that the departure of ZO-2 from the nucleus is regulated by phosphorylation of NES-1 at Ser369.

Novel Protein Kinase Cε Regulates the Exit of ZO-2 from the Nucleus

We next analyzed which PKC isoforms modulate the nuclear exportation of ZO-2, by using several PKC inhibitors. For Gö 6976 and rottlerin, the earliest time point at which the drugs could be added was 10 h after transfection (4 h in Figure 5), because an earlier addition triggered the detachment of the recently transfected cells from the coverslips. Figure 5 reveals how treatment with 150 nM Gö 6976 (triangles), which is known to inhibit cPKCα and -β1 and the nPKCμ, exerts no effect in comparison with monolayers treated with 0.1% DMSO vehicle (squares). Instead, cultures treated with 100 nM Ro 318220 (diamond), which inhibits cPKCα, -β1, -β2, and -γ and nPKCε, exhibit a percentage of

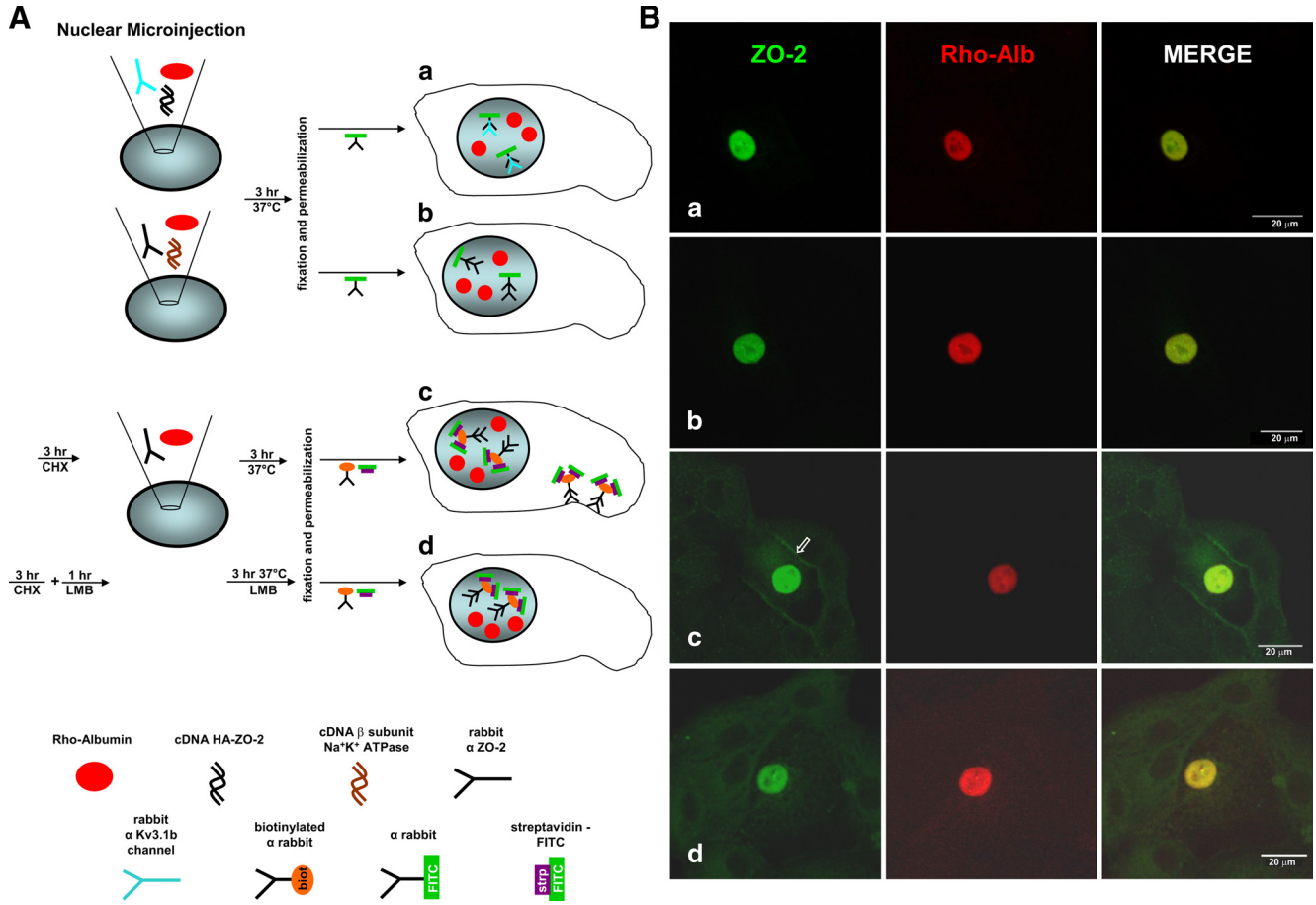

Figure 3. Immunofluorescence patterns obtained with the nuclear microinjection assays designed as negative controls or to study the movement of endogenous ZO-2 from the nucleus to the plasma membrane. (A) Schematic representation of the assays. The sketch illustrates how the nuclei of live MDCK cells were microinjected with rhodaminated albumin and rabbit antibodies against ZO-2 (b–d) or an unrelated rabbit IgG (channel Kv3.1b) (a). In some experiments, a cDNA construct for HA-ZO-2 (a) or a non–ZO-2 cDNA (β subunit of Na^+K^+-ATPase) was microinjected (b). After 3-h incubation at 37°C, the cells were fixed and processed for immunofluorescence with an FITC-coupled antibody against rabbit IgG (a and b) or a biotinylated antibody against rabbit IgG and FITC-coupled streptavidin (c and d). In c and d, the cultures were initially treated for 3 h with 50 μg/ml cycloheximide. In d, the culture was treated with 50 nM LMB 1 h before the microinjection and kept with LMB until the cells were fixed. (B) Immunofluorescence patterns. From a–d, it can be observed that rhodaminated albumin remains confined to the nucleus. In a, in the absence of a specific antibody against ZO-2 microinjected into the nucleus, no ZO-2 stain is observed at the plasma membrane of cells microinjected with the HA-ZO-2 construct. In b, when no HA-ZO-2 cDNA is microinjected into the nucleus, no fluorescence ZO-2 signal is detected at the cell borders. In c, when cells were subjected previously to a 3-h protein synthesis blockade, a faint green stain of endogenous ZO-2 is detected at the plasma membrane (arrow). d, no green staining of endogenous ZO-2 is detected at the cell borders of cells treated with LMB. Note that images in c and d have been taken with a much higher background signal to favor observation of ZO-2 at the cell borders. Rho, rhodamine; Alb, albumin.

cells with nuclear ZO-2 that increases in the first 5 h from 52 to 61% and then remains stable throughout the experiment. We conclude that either cPKCβ2 and -γ or nPKC ε regulate the exportation of ZO-2 from the nuclei.

Because the commercial PKC-permeable inhibitors that affect cPKC β2 and γ also inhibit the nPKC ε, we next decided to use bryostatin 1, because this drug has been shown to induce after 30 min a rapid and sustained activation of nPKC isozymes δ and ε, whereas activation of cPKCα occurs only after 3–4 h followed by down-regulation (Song *et al.*, 2001). Treatment with 200 nM bryostatin 1 produces a decrease in the percentage of cells exhibiting nuclear ZO-2 staining (empty circles), suggesting that activation of either nPKCδ or -ε is stimulating the nuclear exportation of ZO-2.

We next tried rottlerin because it selectively inhibits nPKCδ when used at a concentration of 10 μM (Song *et al.*, 2001). The full circles in Figure 5 reveal that the percentage of cells with nuclear ZO-2 is similar to that found in DMSO-treated monolayers.

Together, these results strongly suggest that nPKCε is phosphorylating the NES-1 signal of ZO-2, thereby allowing the exportation of ZO-2 from the nucleus.

The Phosphorylation of Serine 369 by Novel Protein Kinase Cε Is Critical for the Departure of ZO-2 from the Nucleus

To substantiate the importance of Ser369 for ZO-2 nuclear exportation, we microinjected the nuclei of MDCK cells with the amino segment of ZO-2 in its wild-type form (WT amino-ZO-2-GST) or containing the mutation S369A (Figure 6A). Figure 6B, a and b, shows how, as reported previously (Gonzalez-Mariscal *et al.*, 2006), the microinjected WT amino-ZO-2-GST protein exits the nucleus in a LMB-sensitive way. Now, we show that the microinjected amino-ZO-2-GST

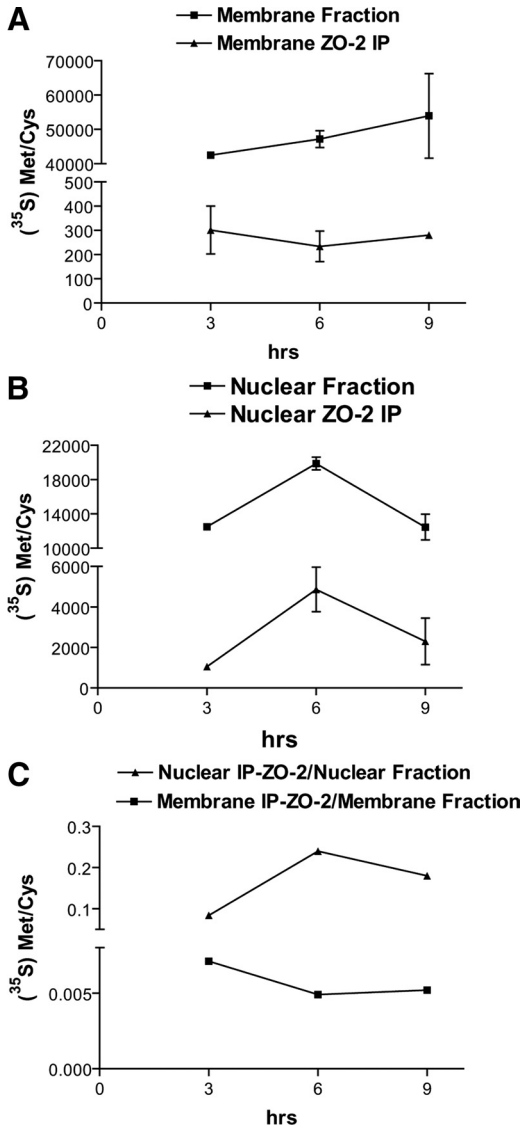

Figure 4. A higher amount of newly synthesized endogenous ZO-2 reaches the nucleus than the plasma membrane. Cultures subjected to a 3-h protein synthesis blockade by incubation with cycloheximide were next washed and subjected to 3-, 6-, and 9-h pulses of [^{35}S]Met/Cys. Monolayers were treated with lysis buffer, and nuclear and membrane fractions were isolated. We used 250 μg of each cell fraction for ZO-2 immunoprecipitation. The radioactive counts present in 250 μg of nuclear and membrane fractions and in the ZO-2 IP derived from them were determined in a scintillation counter. (A) Plasma membrane fraction and ZO-2 IP from plasma membrane fraction. (B) Nuclear fraction and ZO-2 IP from nuclear fraction. (C) Ratios of nuclear ZO-2 IP/nuclear fraction and plasma membrane ZO-2 IP/plasma membrane fraction.

protein containing mutation S369A remains concentrated at the nucleus (Figure 6Be), indicating that Ser369 is critical for the nuclear exit of the protein.

To demonstrate the participation of PKC on Ser369 phosphorylation, the cells were microinjected with WT amino-ZO-2-GST protein and the PKC inhibitor peptide 19-36, (Makowske and Rosen, 1989) or a peptide that specifically inhibits nPKCε translocation and function in vivo (Johnson *et al.*, 1996;Brandman *et al.*, 2007). Figure 6B shows how the amino segment of ZO-2 concentrates at the nuclei when PKC (Figure 6Bc) or nPKCε (Figure 6Bd) are inhibited.

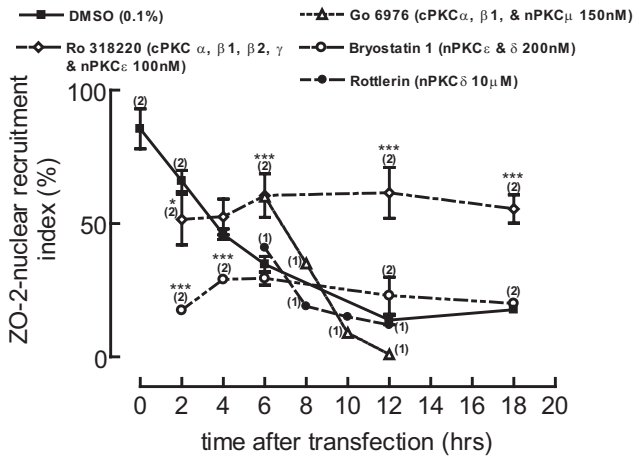

Figure 5. Employment of PKC inhibitors and stimulators indicates the participation of nPKCε in the nuclear exportation of ZO-2. The percentage of cells with nuclear ZO-2 was determined by immunofluorescence using an anti-HA antibody. Monolayers were fixed at the indicated time points. Time zero corresponds to the 6th h after transfection with HA-ZO-2. Monolayers were treated for the last 2 h before fixation at the indicated times, with 0.1% DMSO (full squares), 150 nM Gö 6976 (triangles), 100 nM Ro 318220 (diamonds), 10 μM rottlerin (full circles), or 200 nM bryostatin 1 (empty circles). *$p < 0.05$; **$p < 0.005$; and ***$p < 0.0005$, determined by a Fisher exact test comparing experimental to control values.

Novel Protein Kinase Cε Coimmunoprecipitates with Native ZO-2 But Not with a Mutant Lacking Ser369

To confirm the interaction of nPKCε with ZO-2, we searched for the presence of nPKCε in ZO-2 immunoprecipitates derived from sparse cells transfected previously with wild-type ZO-2 (HA-ZO-2), a mutant ZO-2 lacking Ser369 (HA-ZO-2 Mut. S369A), or the empty vector (pGW1). Figure 7 reveals that nPKCε coimmunoprecipates with wild-type ZO-2 but not with the mutant that lacks Ser369. Instead, cPKCβ2, coimmunoprecipitates with both wild-type ZO-2 and the S369A mutant. This last observation was expected and taken as a positive control, because we had demonstrated previously the interaction of cPKCβ with the middle and carboxy segments of ZO-2 (Avila-Flores *et al.*, 2001).

Novel Protein Kinase Cε Phosphorylates the Amino Segment of ZO-2 That Contains an Intact Ser369 Residue

Next, we explored through an in vitro phosphorylation assay, whether the amino-ZO-2 segment requires the presence of Ser369 to be efficiently phosphorylated by nPKCε. Figure 8A shows a representative autoradiography with its corresponding dried and Coomassie Blue-stained gel. As it can be observed, the typical PKC substrate histone H1 and the wild-type amino-ZO-2-GST fusion protein are nPKCε phosphorylation targets but not the amino-ZO-2-GST S369A mutant. In addition, Figure 8B reveals that whereas the specific phosphorylation of mutant S369A is not sensitive to PKCε stimulation with bryostatin 1 (black bar) with respect to control (gray bar), WT amino-ZO-2-GST protein phosphorylation increases upon treatment with bryostatin 1 (black bar) and is blocked with Ro 318220 (empty bar). These results thus indicate that in ZO-2, Ser369 is a target of nPKCε phosphorylation.

DISCUSSION

Here, we have studied the destiny of newly synthesized ZO-2. To achieve this purpose, we followed by immunoflu-

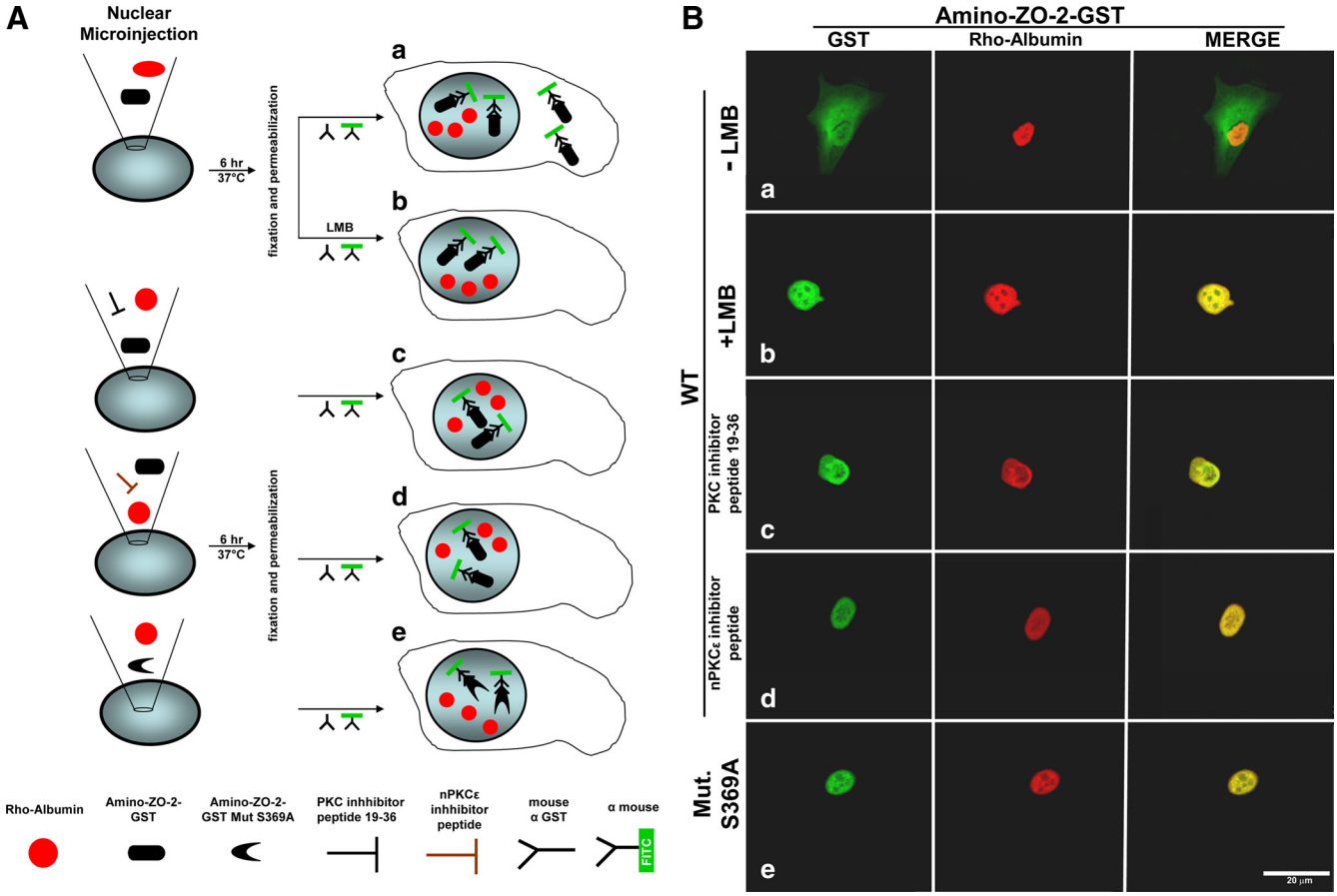

Figure 6. The nuclear export of the amino-ZO-2 segment is blocked by treatment with LMB, upon S369A mutation and by the inhibition of nPKCε activation. (A) Schematic representation of the assay. The sketch illustrates how the nuclei of live MDCK cells were microinjected with rhodaminated albumin (a–e), the GST fusion proteins amino-ZO-2 (a–d) or amino-ZO-2 Mut. S369A (e), the PKC inhibitor peptide 19-36 (c), or the nPKCε translocation/activation inhibitor peptide (d). After 6-h incubation at 37°C, the cells were fixed and processed for immunofluorescence with a mouse antibody against GST and a secondary FITC-coupled antibody against mouse IgG. In b, the culture was treated with 50 nM LMB. (B) Immunofluorescence patterns obtained. From a–e, rhodaminated albumin remained confined to the nucleus. In a, observe how microinjected amino-ZO-2-GST has been exported from the nucleus and now also stains the cytoplasm. Instead, amino-ZO-2-GST remains confined to the nucleus when the cells are treated with LMB (b), a PKC inhibitor peptide (c), a specific nPKCε activation inhibitor (d); or are microinjected with amino-ZO-2-GST with the mutation S369A. Rho, rhodamine.

orescence observation at different time points, the subcellular distribution of ZO-2–transfected into sparse MDCK cells. Our results indicate that immediately after the 6-h period of transfection, 74% of transfected cells have ZO-2 at the nucleus and that this percentage diminishes 18 h later to 17%. This change seems to be due to the exit of ZO-2 from the nucleus because the process is sensitive to LMB. Although

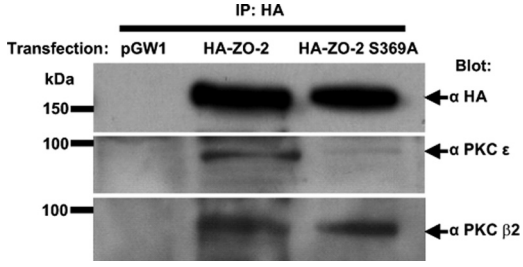

Figure 7. Association of nPKCε to ZO-2 depends on the presence of Ser369. HA immunoprecipitates derived from MDCK cells transfected with HA-ZO-2 or HA-ZO-2 Mut. S369A were blotted with antibodies against HA, nPKCε, or cPKCβ2.

ZO-2 has four functional NESs (Jaramillo *et al.*, 2004;Gonzalez-Mariscal *et al.*, 2006), we have previously demonstrated that the mutation of a single NES is sufficient to induce a strong nuclear accumulation of the protein (Gonzalez-Mariscal *et al.*, 2006). Based on this fact and on the observation that NES-1 contains a Ser within a PKC phosphorylation consensus site, we explored whether the exit of nuclear ZO-2 could be hampered replacing Ser369 for Ala. To our surprise, we first observed that at time 0, the percentage of cells with nuclear ZO-2 is significantly lower in the cultures transfected with ZO-2 mutant S369A than in cells transfected with wild-type ZO-2. We do not have a clear explanation for this behavior. Next and in agreement with our expectations, we observed that when the cultures were transfected with ZO-2 Mut. S369A, the percentage of cells with nuclear ZO-2 instead of decreasing, augmented with time after transfection. These results hence support the idea that after synthesis ZO-2 travels to the nucleus and is exported from this compartment at a later stage through a process that requires the NESs of the molecule.

Previously, we had demonstrated that nPKCε phosphorylates ZO-2 and coimmunoprecipitates with this TJ protein

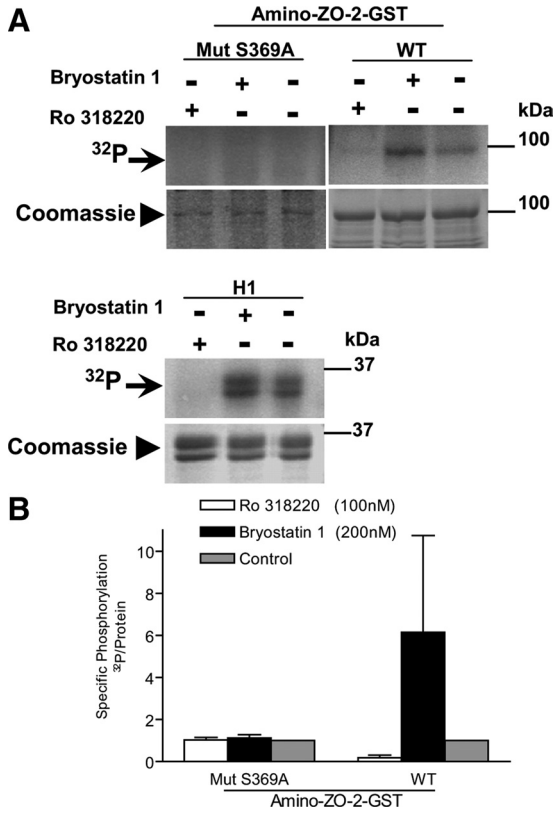

Figure 8. Mutant S369A amino segment of ZO-2 is not responsive to phosphorylation mediated by nPKCε. nPKCε immunoprecipitates were incubated with histone H1 or the GST fusion proteins amino-ZO-2 WT or the Mut. S369A. The assay was performed with [$^{32}\gamma$-P]ATP in the presence of kinase activators phosphatidylserine and 1,2-diolein, with and without the novel and classic PKC inhibitor Ro 318220 and the nPKC ε and δ stimulator bryostatin 1. The arrowheads and arrows, respectively, denote the amino-GST fusion proteins and histone H1 in the ^{32}P autoradiography (A, top) and Coomassie-stained gel (A, bottom). (B) Specific phosphorylation of amino-ZO-2-GST fusion proteins Mut. S369A and WT by nPKCε. [^{32}P]Phosphate labeling of the bands corresponding to amino-ZO-2-GST fusion proteins Mut. S369A and WT were detected by autoradiography, and the amount of these proteins loaded was determined in the same gel by staining with Coomassie Blue. Autoradiography and Coomassie Blue staining gels were quantified with an image densitometer and the specific phosphorylation was determined as the ratio of phosphorylated protein to the total protein content. Control phosphorylation (without PKC stimulators and inhibitors) was taken as 1 to normalize the results of at least three independent experiments. Results are means ± SD. H1, histone H1.

only if the culture is subconfluent (Avila-Flores *et al.*, 2001), a condition in which ZO-2 is present at the nucleus (Islas *et al.*, 2002). In addition, others had demonstrated that nPKCε is present at the nuclei of MDCK cells (Dodane and Kachar, 1996). Here, we show that the association of ZO-2 with nPKCε, the phosphorylation of the amino-ZO-2 segment by this PKC isozyme, as well as the departure of the amino-ZO-2-GST protein from the nucleus, are critically dependent upon the presence of Ser369. We also show that the stimulation of nPKCε by bryostatin 1 inhibits the accumulation of ZO-2 at the nucleus and augments the phosphorylation of amino-ZO-2-GST fusion protein, whereas the inhibition of nPKCε with the translocation inhibitor peptide blocks the export of the nuclear microinjected amino-ZO-2-GST protein. These results strongly suggest that the nuclear exportation of ZO-2 is mediated by nPKCε phosphorylation of NES-1 at Ser369.

To analyze whether ZO-2 present at the TJ had previously made a stopover at the nucleus, we devised a novel assay in which the nucleus functioned as a reservoir for antibody against ZO-2. Because the size of antibodies is higher than that required for free diffusion of molecules from the nucleus, ZO-2 present at the cell borders could only render an immunofluorescent signal if the protein had interacted previously with the antibody at the nucleus. The results of this assay reveal a clear cell border staining of transfected ZO-2 that is abolished when the culture is pretreated with LMB, indicating that newly synthesized ZO-2 goes into the nucleus and is later relocated to the plasma membrane. These experiments, however, cannot rule out the possibility that a small portion of newly synthesized ZO-2 goes directly to the plasma membrane without making a stopover at the nucleus.

Considering the possibility that the number of ZO-2 binding sites at the cell borders may be already occupied by endogenous ZO-2, we devised an experiment in which the localization of endogenous ZO-2 was studied in cells subjected previously to a protein synthesis blockade. By immunofluorescence, a faint but yet detectable signal of ZO-2 was found at the cell borders indicating that endogenous ZO-2 had been delivered to the nucleus before reaching the plasma membrane. In addition, the biosynthetic labeling experiments demonstrated that in sparse cultures, a higher amount of newly synthesized ZO-2 is found at the nucleus than at the plasma membrane. The fact that the amount of newly synthesized ZO-2 found at the membrane does not change with 3-, 6-, and 9-h [^{35}S]Met/Cys pulses, suggests that the number of ZO-2 binding sites at the TJ region are limited. Instead, the considerably higher and variable amount of newly synthesized ZO-2 present at the nucleus, favors the idea of considering the nucleus a cellular reservoir for ZO-2.

In summary, our results indicate that ZO-2 can make a stopover at the nucleus before reaching the plasma membrane and that export of ZO-2 from the nucleus is regulated by the phosphorylation of NES-1 at Ser369 by nPKCε.

ACKNOWLEDGMENTS

This work was supported by Mexican Consejo Nacional de Ciencia y Tecnologia (CONACYT) grants 45691-Q (to L.G.-M.) and 54756 (J. S.) and by a multidisciplinary grant from CINVESTAV. D. C. and R. T. were recipients of doctoral fellowships 165787 and 166727 from CONACYT.

REFERENCES

Avila-Flores, A., Rendon-Huerta, E., Moreno, J., Islas, S., Betanzos, A., Robles-Flores, M., and Gonzalez-Mariscal, L. (2001). Tight-junction protein zonula occludens 2 is a target of phosphorylation by protein kinase C. Biochem. J. *360*, 295–304.

Brandman, R., Disatnik, M. H., Churchill, E., and Mochly-Rosen, D. (2007). Peptides derived from the C2 domain of protein kinase C epsilon (epsilon PKC) modulate epsilon PKC activity and identify potential protein-protein interaction surfaces. J. Biol. Chem. *282*, 4113–4123.

Dodane, V., and Kachar, B. (1996). Identification of isoforms of G proteins and PKC that colocalize with tight junctions. J. Membr. Biol. *149*, 199–209.

Gonzalez-Mariscal, L., Betanzos, A., and Avila-Flores, A. (2000a). MAGUK proteins: structure and role in the tight junction. Semin. Cell Dev. Biol. *11*, 315–324.

Gonzalez-Mariscal, L., Chavez, d. R., and Cereijido, M. (1985). Tight junction formation in cultured epithelial cells (MDCK). J. Membr. Biol. *86*, 113–125.

Gonzalez-Mariscal, L., Namorado, M. C., Martin, D., Luna, J., Alarcon, L., Islas, S., Valencia, L., Muriel, P., Ponce, L., and Reyes, J. L. (2000b). Tight

junction proteins ZO-1, ZO-2, and occludin along isolated renal tubules. Kidney Int. *57*, 2386–2402.

Gonzalez-Mariscal, L., Ponce, A., Alarcon, L., and Jaramillo, B. E. (2006). The tight junction protein ZO-2 has several functional nuclear export signals. Exp. Cell Res. *312*, 3323–3335.

Gumbiner, B., Lowenkopf, T., and Apatira, D. (1991). Identification of a 160-kDa polypeptide that binds to the tight junction protein ZO-1. Proc. Natl. Acad. Sci. USA *88*, 3460–3464.

Islas, S., Vega, J., Ponce, L., and Gonzalez-Mariscal, L. (2002). Nuclear localization of the tight junction protein ZO-2 in epithelial cells. Exp. Cell Res. *274*, 138–148.

Itoh, M., Furuse, M., Morita, K., Kubota, K., Saitou, M., and Tsukita, S. (1999a). Direct binding of three tight junction-associated MAGUKs, ZO-1, ZO-2, and ZO-3, with the COOH termini of claudins. J. Cell Biol. *147*, 1351–1363.

Itoh, M., Morita, K., and Tsukita, S. (1999b). Characterization of ZO-2 as a MAGUK family member associated with tight as well as adherens junctions with a binding affinity to occludin and alpha catenin. J. Biol. Chem. *274*, 5981–5986.

Jaramillo, B. E., Ponce, A., Moreno, J., Betanzos, A., Huerta, M., Lopez-Bayghen, E., and Gonzalez-Mariscal, L. (2004). Characterization of the tight junction protein ZO-2 localized at the nucleus of epithelial cells. Exp. Cell Res. *297*, 247–258.

Johnson, J. A., Gray, M. O., Chen, C. H., and Mochly-Rosen, D. (1996). A protein kinase C translocation inhibitor as an isozyme-selective antagonist of cardiac function. J. Biol. Chem. *271*, 24962–24966.

Kudo, N., Wolff, B., Sekimoto, T., Schreiner, E. P., Yoneda, Y., Yanagida, M., Horinouchi, S., and Yoshida, M. (1998). Leptomycin B inhibition of signal-mediated nuclear export by direct binding to CRM1. Exp. Cell Res. *242*, 540–547.

Makowske, M., and Rosen, O. M. (1989). Complete activation of protein kinase C by an antipeptide antibody directed against the pseudosubstrate prototope. J. Biol. Chem. *264*, 16155–16159.

Mattagajasingh, S. N., Huang, S. C., Hartenstein, J. S., and Benz, E. J., Jr. (2000). Characterization of the interaction between protein 4.1R and ZO-2. A possible link between the tight junction and the actin cytoskeleton. J. Biol. Chem. *275*, 30573–30585.

Metais, J. Y., Navarro, C., Santoni, M. J., Audebert, S., and Borg, J. P. (2005). hScrib interacts with ZO-2 at the cell-cell junctions of epithelial cells. FEBS Lett. *579*, 3725–3730.

Robles-Flores, M., Rendon-Huerta, E., Gonzalez-Aguilar, H., Mendoza-Hernandez, G., Islas, S., Mendoza, V., Ponce-Castaneda, M. V., Gonzalez-Mariscal, L., and Lopez-Casillas, F. (2002). p32 (gC1qBP) is a general protein kinase C (PKC)-binding protein; interaction and cellular localization of P32-PKC complexes in ray hepatocytes. J. Biol. Chem. *277*, 5247–5255.

Shoshani, L., Contreras, R. G., Roldan, M. L., Moreno, J., Lazaro, A., Balda, M. S., Matter, K., and Cereijido, M. (2005). The polarized expression of Na+,K+-ATPase in epithelia depends on the association between beta-subunits located in neighboring cells. Mol. Biol. Cell *16*, 1071–1081.

Song, J. C., Hanson, C. M., Tsai, V., Farokhzad, O. C., Lotz, M., and Matthews, J. B. (2001). Regulation of epithelial transport and barrier function by distinct protein kinase C isoforms. Am. J. Physiol. Cell Physiol. *281*, C649–C661.

Tapia, R., Huerta, M., Islas, S., Avila-Flores, A., Lopez-Bayghen, E., Weiske, J., Huber, O., and Gonzalez-Mariscal, L. (2009). Zona occludens-2 inhibits cyclin D1 expression and cell proliferation and exhibits changes in localization along the cell cycle. Mol. Biol. Cell *20*, 1102–1117.

Traweger, A., Fuchs, R., Krizbai, I. A., Weiger, T. M., Bauer, H. C., and Bauer, H. (2003). The tight junction protein ZO-2 localizes to the nucleus and interacts with the heterogeneous nuclear ribonucleoprotein scaffold attachment factor-B. J. Biol. Chem. *278*, 2692–2700.

Wittchen, E. S., Haskins, J., and Stevenson, B. R. (1999). Protein interactions at the tight junction. Actin has multiple binding partners, and ZO-1 forms independent complexes with ZO-2 and ZO-3. J. Biol. Chem. *274*, 35179–35185.